Dynamic Changes of Pulmonary Veins Ostia in Controls and Atrial Fibrillation Patients

Matteo Falanga[1], Giulio Molon[2], Carmelo Cicciò[2], Stefano Bonapace[2], Cristiana Corsi[1]

[1]DEI, University of Bologna, Campus of Cesena, Bologna, Italy
[2]IRCCS Sacro Cuore Don Calabria Hospital, Negrar, Verona, Italy

Abstract

The quantitative evaluation of pulmonary veins (PVs) contraction and its connection with atrial fibrillation (AF) have not yet been clearly defined. The purpose of this study was to investigate the variation of PVs ostial size using ECG-gated cardiac CECT (contrast enhanced computed tomography) as this modality may be useful for monitoring patients after PVs isolation procedures. Analysis was performed on 9 control (CTRL) patients, 9 paroxysmal AF (PAR) patients and 9 persistent AF (PER) patients (mean age 61 ± 10 years, 23 males and 4 females). The left atrium (LA) anatomical model was reconstructed throughout the cardiac cycle and the PVs ostial area and their variation was obtained. As a result, the inferior veins were found to be the smallest on average, on the left side particularly, while the right superior vein was found to be the biggest. The same results were found for the PVs ostial area variation, which was the lowest for the inferior veins and the biggest for the right superior vein. Morphological and functional differences were found among the groups. AF patients had lower PVs ostial area variation compared to controls, highlighting a reduction in effectiveness in terms of passive filling and active contraction within the LA that makes the PVs ostia contracting less than in healthy subjects.

1. Introduction

Atrial fibrillation (AF) is the most common arrhythmia in clinical practice. It can occur at any age but is very rare in children and becomes extremely common in the elderly, with a prevalence approaching 20% in patients > 85 years of age [1]. Its consequences involve increased risk of death, increased thromboembolic events as well as decreased quality of life [2].

Over the past years, the treatment of AF using a PV isolation approach has emerged from being a highly experimental procedure to a procedure performed in many electrophysiology laboratories [3-5]. One of the most important discoveries in this context has been that PVs play a prominent role in the pathogenesis of AF [6,7] and thus the mechanistic link between PVs and AF has been the subject of intense interest [8]. There are theories that AF can be predicted by both histological characteristics and the gross morphology of PVs ostia [9,10].

Our understanding of AF pathophysiology has advanced significantly over the past 10 to 15 years through an increased awareness of the role of "atrial remodeling." Any persistent change in atrial structure or function constitutes atrial remodeling [11]. Pathological examination has demonstrated the existence of muscle fibers arranged in a circular pattern around the PVs ostia, and of layers of atrial muscle extending up to several centimeters into the pulmonary veins [12]. It was assumed that these circumferential layers of atrial muscle may work as a sphincter-like mechanism, preventing backflow of blood during atrial contraction [13], as also that the layers of myocardium inside the PVs are the triggers of AF in most patients with paroxysmal AF [3]. However, it cannot be excluded that a contraction occurs not only at the ostia, but also more distally [14].

Our hypothesis is that ECG-gated cardiac CECT would allow non-invasive evaluation of PVs contraction patterns. This could be helpful for assessing patients after PV ablation, as the lack of PV contraction might serve as a stand-in indicator of effective PV isolation.

2. Methods

2.1. Patients data

The data utilized in this investigation were obtained thanks to a collaboration with Sacro Cuore Don Calabria Hospital, Negrar, Verona. In compliance with the Helsinki Declaration, all subjects provided written informed consent.

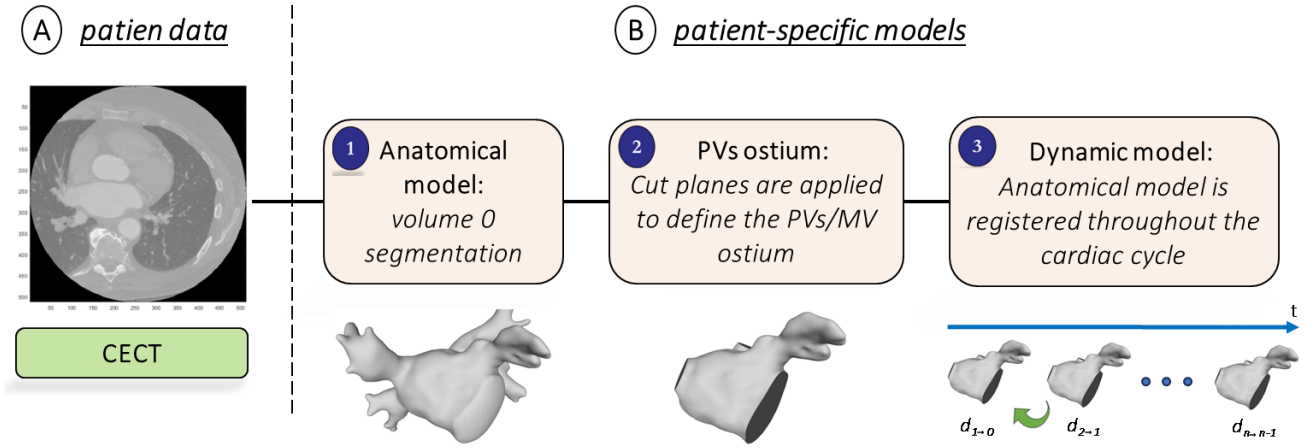

Figure 1. Workflow of the study: patient-specific contrast enhanced CT (CECT) data are processed to derive the LA anatomical model (B1). Cut planes are applied on the latter to define the PVs ostia (B2). The new model is used to perform the registration throughout the cardiac cycle (B3), with n the number of volumes acquired.

Only patients with a standard anatomy (four PVs, two on the left and two on the right) were selected for the study. To carry out this study, 18 patients with AF were included retrospectively, along with a control group of 9 patients with normal heart structure and no previous history of AF.

CT dynamic acquisitions of the heart after contrast medium injection were performed in each patient utilizing a 64-slice multi-detector CT scanner (Philips Brilliance 64 CT scanner) with retrospective ECG gating during normal sinus rhythm.

From ventricular end diastole, volumetric CT images were reconstructed for a total of 10 phases. Each CT volume was 512x512x200 pixels. The voxel resolution was not isotropic: 0.39 mm on x-y plane and 1 mm of slice thickness, yielding a voxel size of 0.39x0.39x1 mm^3.

2.2. Data analysis

The process to analyze CT data is depicted in Figure 1 and includes several steps that are described in this section.

The first volume acquired for each patient during the cardiac cycle was segmented using an active contour algorithm featured on ITK-SNAP (version 3.8.0, Kitware Inc.). This algorithm initially focused on segmenting the LA including left atrial appendage (LAA) by defining a region of interest. The operator manually selected a seed, which guided the algorithm to grow towards the LA wall and enclose the entire LA anatomy, including the LAA. In order to improve the initial segmentation, its contour was regularized and smoothed using morphological operators and a Laplacian filter, respectively. Finally, the result was exported as a stereolithography file. This entire procedure was executed solely on the first obtained volume of each dynamic dataset.

Through the use of Paraview (version 5.10.1, Kitware Inc.), cut planes were applied to delineate the ostia of the PVs. These planes were positioned in accordance with the anatomical ostia of the veins (Figure 2).

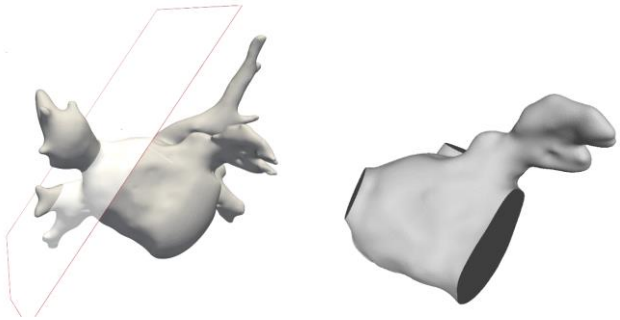

Figure 2.Second step of the workflow. The use of the cut plane on the RSPV is seen on the left. The final product with all the cut planes applied is seen on the right.

Because the cut alters the structure of the surface faces by removing portions of them and attached nodes, the entire surface was remeshed so that the newly established boundaries had new nodes. This was necessary to improve the performance and, consequently, the result of the next step.

First, a rigid transformation was applied for an initial alignment, and then subsequently transitioned to an affine registration. The result has been further refined applying a 3D non-rigid registration based on a B-spline transformation model [15] with the mean square difference as cost function. For additional details regarding the registration phase, readers should refer to [16]. The dynamic surfaces were now accessible for additional investigation for each dataset. Matlab was used to calculate the area of the PVs by loading the whole dynamic dataset of surfaces for each patient. To do so, the barycenter of each boundary was employed as a reference, as shown in Figure 3. The applied formula is simply the area of the triangle as the sum of all triangles inside the boundary:

$$PVarea = \sum_{i=1}^{n} \frac{1}{2} \|(B_i - A)\ x\ (B_{i+1} - A)\|$$

where A is the barycenter of the corresponding PV and B are the points on the boundary. This formula is applied iteratively for each PV.

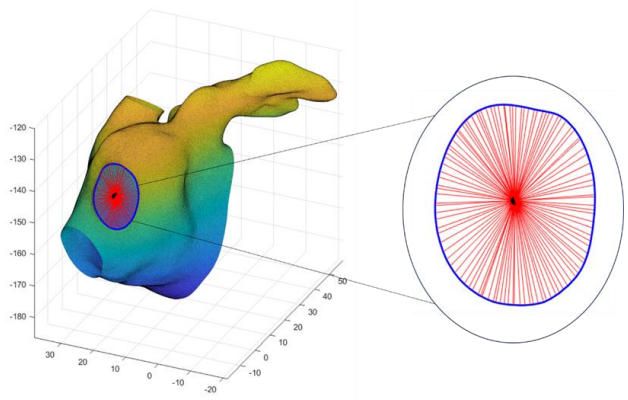

Figure 3. On the left, a septal/anterior view of the left atrium with the RSPV (Right superior pulmonary vein) highlighted. On the right, a close-up of the RSVP where the connections between each node on the boundary and the barycenter are clearly visible.

The final result is a PV area curve that represent the entire cardiac cycle for each patient. An example is shown in Figure 4. In addition, the percentage area variation of each PV is calculated as follows:

$$Area\ \% = \left(\frac{Area_{max} - Area_{min}}{Area_{max}}\right) * 100$$

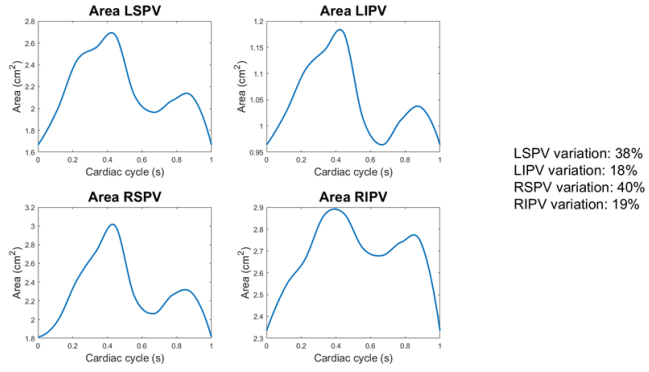

Figure 4. Pulmonary veins area curves throughout the cardiac cycle (from 0 to 1s). LSPV (Left superior pulmonary vein), LIPV (Left inferior pulmonary vein), RSPV (Right superior pulmonary vein), RIPV (Right inferior pulmonary vein). On the right, the percentage area variation for each PV.

3. Results

In total, 27 patients were analyzed. The mean age was 61 ± 10 and 23 patients were males and 4 females.

The use of 3D LA anatomical models derived from CECT acquisitions enabled the accurate visualization of the structure and identification of the ostia of PVs.

When examining the area of the PVs, it was found that both the left superior pulmonary vein (LSPV) and the right superior pulmonary vein (RSPV) were notably larger in the PER group ($p = 0.024$ and $p = 0.049$ respectively) compared to PAR and CTRL groups. In general, it was observed that the PVs appeared to be larger in the patients with AF when compared to the patients in the control group.

By considering the entire PVs area curve, the percentage area variation was determined by applying the formula outlined in subsection 2.2. The right inferior pulmonary vein (RIPV) exhibited less contraction compared to the other PVs, higher in the CTRL group (20 ± 6 %) as compared to PAR (14 ± 6 %) and PER (10 ± 4 %). On the contrary, the RSPV and LSPV showed higher contraction percentages in the CTRL group (42 ± 11% and 39 ± 6% respectively) compared to the PAR group (28 ± 7% and 24 ± 9%) and PER group (16 ± 7% and 15 ± 6%). Overall, it was observed that the contraction was more pronounced in the control patients compared to those with AF.

4. Discussion

The patients included in this study are characterized by the most common LA anatomy (four PVs, two on the left and two on the right). It was seen that PVs area curves approximately follow the LA contraction. The LSPV and RSPV, particularly in the CTRL group, showed the greatest contraction among the PVs. In addition, the same PVs were found to be the largest, especially in the PER group. These results show that CECT acquisitions can be used to assess PVs contraction.

It is possible that the contraction observed in this study is a consequence of an incorrect identification of the PVs ostia since the cut planes were manually applied only by considering the visible anatomical ostia, resulting in measurements of the contraction in the atrial tissue. On the other hand, assuming the ostia identification is correct, the observed contraction could be due to the circular arrangement of muscle fibers around the ostia and within the PV, compression from nearby structures, LA filling phase, or contraction of the LA antral region, which will enclose the proximal part of the PV as a prevention of backflow. The decrease in area observed after about 40 % of the cardiac cycle can be supposed to be a passive process caused by decreased blood flow in

the veins and opening of the mitral valve, while the second decrease in area around 80/85 % of the cardiac cycle can reasonably be attributed it to the active contraction of the atrium. Regarding a possible compression caused by external factors, it is true that the PVs are close to structures such as the pulmonary arteries and the aorta, but these are normally expanding at different times as compared to the smallest PVs size recorded. The limitation of this study is that it only assess CECT images to reconstruct the 3D LA anatomical model and measure the area of the PVs ostia. Although it has not yet been proven that this imaging modality can be used to compare the contraction of PVs before and after ablation, Thiagalingam et al. [14] proved that the resolution of 64-slice computed tomography is sufficient to detect changes in PVs ostial size.

5. Conclusions

The PVs area curves found were consistent with the LA volume variation throughout the cardiac cycle. The maximal size of the PVs occurs at about 40 % of the cardiac cycle while the minimal size at 85 %. This result is in line with the electrical propagation from the atrial septum. The inferior veins exhibited less contraction while the superior veins showed a higher contraction. When comparing the groups, it was discovered that the CTRL group had the highest PVs contraction while the PAR group had the lowest.

To evaluate the robustness of PV isolation procedures, non-invasive assessment of PVs contraction could be helpful but further data and tests are required to draw any conclusions.

Acknowledgments

This work was supported by the Italian Ministry of University and Research (Italian National Project, PRIN2017 ('Modeling the heart across the scales').

References

[1] Heeringa J, van der Kuip DA, Hofman A, Kors JA, van Herpen G, Stricker BH, Stijnen T, Lip GY, Witteman JC. Prevalence, incidence and lifetime risk of atrial fibrillation: the Rotterdam study. Eur Heart J. 2006; 27: 949–953.

[2] Jais P, Haissaguerre M, Shah DC, et al. A focal source of atrial fibrillation treated by discrete radiofrequency ablation. Circulation. 1997; 95: 572–576.

[3] Haissaguerre M, Jais P, Shah DC, et al. Spontaneous initiation of atrial fibrillation by ectopic beats originating in the pulmonary veins. N Engl J Med. 1998; 339: 659–666.

[4] Chen SA, Hsieh MH, Tai CT, et al. Initiation of atrial fibrillation by ectopic beats originating from the pulmonary veins: electrophysiological characteristics, pharmacological responses, and effects of radiofrequency ablation. Circulation. 1999; 100: 1879–1886.

[5] Haissaguerre M, Shah DC, Jais P, et al. Electrophysiological breakthroughs from the left atrium to the pulmonary veins. Circulation. 2000; 102: 2463–2465.

[6] Mahida S, Sacher F, Derval N, Berte B, Yamashita S, Hooks D, Denis A, Amraoui S, Hocini M, Haissaguerre M, Jais P. Science Linking Pulmonary Veins and Atrial Fibrillation. Arrhythm Electrophysiol Rev. 2015 May;4(1):40-3. doi: 10.15420/aer.2015.4.1.40. Epub 2015 May 30. PMID: 26835098; PMCID: PMC4711542.

[7] Fynn SP, Kalman JM. Pulmonary veins. Pacing Clin Electrophysiol. 2004;27(11):1547–1559. doi: 10.1111/j.1540-8159.2004.00675.x.

[8] Cronin P, Kelly AM, Desjardins B, Patel S, Gross BH, Kazerooni EA, et al. Normative Analysis of pulmonary vein drainage patterns on multidetector CT with measurements of pulmonarry vein ostial diameter and distance to first bifurcation. Acad Radiol. 2007;14(2):178–188. doi: 10.1016/j.acra.2006.11.004.

[9] Khan R. Identifying and understanding the role of pulmonary vein activity in atrial fibrillation. Cardiovasc Res. 2004;64(3):387–394. doi: 10.1016/j.cardiores.2004.07.025.

[10] Lin W-S, Prakash VS, Tai C-T, Hsieh M-H, Tsai C-F, Yu W-C, et al. Pulmonary vein morphology in patients with paroxysmal atrial fibrillation initiated by ectopic beats originating from the pulmonary veins. Implications for catheter ablation. Circulation. 2000;101:1274–1281. doi: 10.1161/01.CIR.101.11.1274.

[11] Nattel S, Burstein B, Dobrev D. Atrial remodeling and atrial fibrillation: mechanisms and implications. Circ Arrhythm Electrophysiol. 2008 Apr;1(1):62-73. doi: 10.1161/CIRCEP.107.754564. PMID: 19808395.

[12] Ho SY, Cabrera JA, Tran VH, et al. Architecture of the pulmonary veins: relevance to radiofrequency ablation. Heart (British Cardiac Society) 2001;86(3):265–270.

[13] Nathan H, Eliakim M. The junction between the left atrium and the pulmonary veins. An anatomic study of human hearts. Circulation. 1966;34(3):412–422.

[14] Thiagalingam A, Reddy VY, Cury RC, Abbara S, Holmvang G, Thangaroopan M, Ruskin JN, d'Avila A. Pulmonary vein contraction: characterization of dynamic changes in pulmonary vein morphology using multiphase multislice computed tomography scanning. Heart Rhythm. 2008 Dec;5(12):1645-50. doi: 10.1016/j.hrthm.2008.09.010. Epub 2008 Sep 7. PMID: 19084798; PMCID: PMC2633604.

[15] M. Unser, "Splines: A perfect fit for signal and image processing," IEEE Signal Process. Mag., vol. 16(6), no. NOVEMBER, pp. 22–38, 1999.

[16] A. Masci et al., "A Proof of concept for computational fluid dynamic analysis of the left atrium in atrial fibrillation on a patient-specific basis," J. Biomech. Eng., vol. 142, no. 1, pp. 1–11, 2020, doi: 10.1115/1.4044583.

Address for correspondence:

Matteo Falanga
DEI, University of Bologna,
Via dell'Università 50, 47522 Cesena (FC), Italy
matteo.falanga2@unibo.it